Fabrication of Elastin−Like Polypeptide Nanoparticles for Drug Delivery by Electrospraying

ARTICLE *in* BIOMACROMOLECULES · JANUARY 2009

Impact Factor: 5.75 · DOI: 10.1021/bm801033f · Source: PubMed

5 AUTHORS, INCLUDING:

John Andrew Mackay
University of Southern California
49 PUBLICATIONS **3,309** CITATIONS
SEE PROFILE

Jonathan R McDaniel
University of Texas at Austin
26 PUBLICATIONS **648** CITATIONS
SEE PROFILE

Ashutosh Chilkoti
Duke University
292 PUBLICATIONS **15,007** CITATIONS
SEE PROFILE

Robert L Clark
University of Rochester
221 PUBLICATIONS **2,707** CITATIONS
SEE PROFILE

Published in final edited form as:
Biomacromolecules. 2009 January 12; 10(1): 19. doi:10.1021/bm801033f.

Fabrication of Elastin-Like Polypeptide Nanoparticles for Drug Delivery by Electrospraying

Yiquan Wu[†,‡], **J. Andrew MacKay**[§], **Jonathan R. McDaniel**[§], **Ashutosh Chilkoti**[*,†,§], and **Robert L. Clark**[*,†,‡]
Center for Biologically Inspired Materials and Material Systems, Duke University, Durham, North Carolina 27708, Department of Mechanical Engineering and Materials Science, Pratt School of Engineering, Duke University, Durham, North Carolina 27708, and Department of Biomedical Engineering, Duke University, 136 Hudson Hall, Box 90281, Durham, North Carolina 27708

Abstract

The development of environmentally responsive drug carriers requires new methods for assembling stimuli-responsive nanoparticulates. This communication describes a novel application of electrospray to construct bioresponsive peptide-based particulates, which can encapsulate drugs. These particles are composed from genetically engineered elastin-like polypeptides (ELPs), a biodegradable, biocompatible, and bioresponsive polymer. To generate nanoparticles (300−400 nm in diameter), ELPs and drugs are codissolved in organic solvent, accelerated across a voltage gradient, dried by evaporation during transit, and collected from a target surface. These findings indicate that particle diameter, polydispersity, and morphology are strong functions of the solvent concentration, spraying voltage, and polymer molecular weight. Surprisingly, the loading of drug at 20 w/w% did not influence particle morphology; furthermore, drug release from these particles correlated with the pH-dependent solubility of the parent ELPs. These studies suggest that electrospray is an efficient and flexible method for generating stimuli-responsive drug particles.

1. Introduction

Electrospraying can create particles by applying a uniform electrohydrodynamic force to break up liquids into fine jets[1,2] and is an emerging method for the rapid and high throughput production of nanomeso scale particles of controlled morphology for controlled release drug delivery applications. A major rationale driving nanoparticle drug formulation is to adjust the kinetics of drug distribution in the body, thus improving the efficacy of existing drugs. At a minimum, these nanoparticles must display (1) reliable drug entrapment, (2) uniform particle dimensions, (3) sufficient stability under physiological conditions, (4) adequate release either over time or in response to a stimuli, and (5) biocompatibility. To this end, electrospray encapsulation of drugs into an environmentally responsive peptide matrix offers a unique opportunity to address the requirements of nanoparticle drug delivery. The morphology and size of electrosprayed polymer nanoparticles is strongly influenced by a host of variables that include processing parameters and the material properties of the solution such as polymer composition, molecular weight (MW), the solvent used for polymer dissolution, and the presence and concentration of other cosolutes (such as a drug).[3] In this communication, the

* To whom correspondence should be addressed. E-mail: rclark@duke.edu (R.L.C.); chilkoti@duke.edu (A.C.)..
[†]Center for Biologically Inspired Materials and Material Systems.
[‡]Pratt School of Engineering.
[§]Department of Biomedical Engineering.

effect of electrospray processing conditions (i.e., flow rate, spraying voltage), the molecular weight of polymer and its concentration were investigated on the morphology and size of electrosprayed particles using a well-defined set of monodisperse recombinant biopolymers and doxorubicin (Dox), a cancer chemotherapeutic.[4,5] We demonstrate that electrospraying is a viable method to generate nanomeso scale biopolymer particles of defined morphology, and the release of the drug is controlled by the dissolution of the particles.

We chose recombinant elastin-like polypeptides (ELPs) as the electrosprayed polymer. ELPs are derived from a pentapeptide Val-Pro-Gly-Xaa-Gly (VPGXG) repeat in the amino acid sequence of human tropoelastin, where the "guest residue," Xaa, can be any combination of natural amino acids except proline.[6,7] We selected ELPs for the following reasons: first, ELPs undergo a thermodynamically driven inverse phase transition at a characteristic temperature, above which they phase separate from bulk water.[8] The ELP transition temperature is similar to a lower critical solution temperature (LCST), above which the system separates into a liquid phase and an insoluble coacervate phase. During electrospraying the solvent, water in this case, is rapidly evaporated leading to the formation of a dehydrated particle. We speculated that upon exposure to an aqueous environment in the body, the ability to undergo coacervation would hinder release of Dox if the solution conditions promote the existence of the insoluble phase.[9,10] Second, ELPs are of interest for biomedical applications,[11-13] including drug delivery.[14] A previous report has demonstrated possible applications of ELP particulates, but to date, ELP particles have not been developed for sustained release of an encapsulated therapeutic,[9] exposing a need for efficient processes capable of converting ELPs into micrometer to nanometer diameter particles. Third, ELPs can be produced recombinantly, which allows precise control over the composition and MW,[6,13] variables that are important in controlling not only the phase transition behavior of ELPs but also the electrospraying, drug encapsulation, and drug release processes.

2. Experimental Section

Synthesis of ELPs Materials

Two ELPs with a MW of 17.8 and 70.2 kD, with a guest residue composition of Val/Ile/Glu [1:3:1], were synthesized for this study to examine the effect of polymer MW on the morphology of the electrosprayed particles. The low molecular weight ELPs had the peptide sequence SKGPG(**V**GVPG**I**GVPG**I**GVPG**E**GVPG**I**GVPG)$_8$WPC. The high molecular weight ELP had the peptide sequence SKGPG(**V**GVPG**I**GVPG**I**GVPG**E**GVPG**I**GVPG)$_{32}$-WPC(GGC)$_7$. We selected ELPs containing glutamic acid residues because (1) we speculated that the inclusion of charges would promote formation of nanoparticles in electrospraying via Coulombic repulsion based on our previous observation that highly charged ELP fusion proteins tend to form nanoparticles (as opposed to microparticles during coacervation), and (2) Glu residues convey a strong pH dependence to the transition temperature of the ELP, allowing us to conveniently and systematically examine the effect of LCST under isothermal conditions by modulation of the pH on the release of the encapsulated drug without the need to synthesize a large set of ELPs with different LCSTs.

The ELPs were synthesized by heterologous expression of a plasmid-borne synthetic gene of the ELP in *E. coli*, as described previously.[13] Genes encoding the ELPs were constructed using recursive directional ligation in a modified pUC19 plasmid in TOP10 cells (Invitrogen Corporation, Carlsbad, CA),[13] ligated into a modified pET25b+ vector (Novagen, Madison, WI), expressed in BLR(DE3) cells (Novagen, Madison, WI) and purified by inverse transition cycling.[15,16] Cysteine residues in these ELPs were reduced during purification by ~10 mM tris carboxyethyl phosphine hydrochloride (TCEP; Pierce Biotechnology, Inc., Rockford, IL). The purified polymers used for this study were obtained from multiple batches at yields greater than 100 mg/L bacterial culture. After purification, ELP molecular weight and purity were

determined by capillary electrophoresis using an Experion instrument (Bio-Rad, Hercules, CA). Electrophoresis confirmed a single 26 kD band (98% purity) for the 17.8 kD ELP and a 105 kD band (100% purity) for the 70.2 kD ELP. The observation of increased MW of ELPs is consistent with previous observations that ELPs under electrophoresis run at ~20−40% higher molecular weight than do globular protein standards.13

Fabrication of Nanoparticles

Figure 1 shows a schematic illustration of the electrospraying setup. A 5mL syringe was filled with ELP solution and a syringe pump was used to dispense the solution. The solution was dispensed at set flow rates of 0.05 mL/h and 0.1 mL/h in separate experiments. A high-voltage power supply with a range of 0−30 kV was used to generate an electric field between the nozzle and the collector. ELP particles were electrosprayed onto a collector located at a set distance of 40 cm away from the nozzle tip. A stable cone-jet mode can not always be guaranteed during electrospraying water solution, but several methods have been developed to deal with this challenge, such as using deionized water as solvent,[17] using a sheath of inert gas or vacuum chamber to prevent electrical discharge,[18,19] using a novel electrospraying nozzle with a nonconductive fiber,[20] using a tine silica nozzle with a 20 μm inner diameter,[21] and using AC voltage superimposed on the DC voltage.[22] In this experiment, a ring electrode slightly below the electrospraying nozzle was incorporated to produce a uniform spraying pattern by creating a cylindrical electric field to help atomization.[2]

ELPs Particle Characterization

The morphologies of electrosprayed ELP particles were characterized by a field emission scanning electron microscope (FESEM, FEI XL 30 SEM-FEG) operated at an accelerating voltage of 5 kV and a working distance of 5 mm. The diameters of particles and size distribution were measured using Image J analysis software (NIH). Prior to SEM analysis, the ELP particles were collected on an aluminum disk and sputter-coated with gold.

ELP Thermal Characterization

ELP transition temperatures were characterized over a range of concentrations (5, 10, 25, 50, and 100 μM ELP in phosphate buffer) by raising the temperature at 1 °C/min on a CARY UV–vis spectrophotometer (Varian, Palo Alto, CA). The transition temperature was defined at the maximum first derivative of the optical density at 350 nm.

DOX Release

Each piece of silica was massed and incubated at 37 °C in 200 μL of buffer of a given pH (pH 2.5: 10 mM succinate, 140 mM NaCl; pH 5.5: 10 mM sodium succinate, 140 mM NaCl; pH 7.5: 10 mM Na_2PO_4, 140 mM NaCl). For each time-point, 200 μL was gently removed and replaced with fresh solution. Dox concentration was determined by fluorescence (excitation: 485 nm; emission: 590 nm) using a Victor-3 96-well plate reader (Perkin-Elmer, Waltham, MA) and computed from a standard curve. Standards and samples were quenched in 1:1 v/v 0.1 M sodium phosphate buffer, pH 7.5 prior to measurement. At the end of the study, each piece of silica was washed in pH 7.5 buffer to recover any remaining ELP and Dox.

3. Results and Discussion

Figure 2 shows SEM images of electrosprayed particles generated from ELPs with a molecular weight of 70.2 kD and a solution concentration of 1 w/v% using different spraying voltages and flow rates. Figure 2a–c show the ELP particles produced at a flow rate of 0.05 mL/h and a spraying voltage of 7, 8, and 9 kV, respectively. At a spraying voltage of 7 kV, both particulate and fibrous ELP structures were produced, and the particles were connected by the fibers. As

the spraying voltage increased to 8 kV and greater, particles with fibrous tails were formed. The particle sizes were distributed over a range of 115−680 nm. Figure 2d–f show that when the flow rate of solution was increased to 0.1 mL/h, more fibrous ELP structures were produced. Using a spraying voltage of 7 kV, a predominantly fibrous microstructure was obtained, as shown in Figure 2d. Increasing the spraying voltage from 7 to 9 kV generated more ELP particles and fewer fibers, as shown in Figure 2f. This trend was a result of a shift in the balance of forces on the surface of the charged droplets of ELP solution. As the applied voltage was increased, the electrostatic force more easily overcame the surface tension on the droplets and atomized the charged droplets into particles. Increasing the flow rate of solution drove more precursor materials to be electrosprayed and thus made it easier to generate fiber or tail structures when using high molecular weight polymers.[23,24]

Figure 3 shows SEM images of the morphologies of electrosprayed ELP particles produced using the same parameters as those used to generate the structures shown in Figure 2, with a lower solution concentration of 0.5 w/v%. Reduction of the ELP concentration produced smaller particle sizes (Figure 3). The particle size distribution covered a range of 50−560 nm, but the morphology of the ELP particles was more uniform than that observed for particles produced under other processing conditions. Additionally, lower polymer concentration generated fewer fibers; however, the ELP particles retained tail structures, which were related to the high molecular weight of ELP (vide infra). Compared to the microstructure in Figure 2, the morphologies of ELP particles became smoother and more spherical, and particle tailing became shorter.

To investigate the influence of ELP molecular weight on the formation of particles, an ELP with the same composition but a lower molecular weight of 17.8 kD also was electrosprayed. Figure 4 shows SEM images of the resulting particles using this low molecular weight ELP at a solution concentration of 1 w/v%. Figure 4a–c show microstructures of ELP particles produced at a flow rate of 0.05 mL/hr and at spraying voltages of 7, 8, and 9 kV. The experimental results revealed that the electrosprayed ELP particles were uniform and had spherical and smooth morphologies. The micrographs show very few tail formations. When the flow rate was increased to 0.1 mL/h, spherical ELP particles with larger sizes were generated, as shown in Figure 4d–f. At a spraying voltage of 7 kV, the sizes of electrosprayed ELP particles ranged from 50 to 550 nm, with an average value of 457 nm, while the particle size distribution covered 80−480 nm at a spraying voltage of 8 kV, with an average value of 430 nm. When the spraying voltage increased to 9 kV, the ELP particle sizes varied from 92 to 590 nm, with an average value of 415 nm. The SEM images show that the particles were less agglomerated and had smoother surfaces when the flow rate was increased to 0.1 mL/h. During electrospraying, the flow rate of solution controls the quantity of precursor solution to the tip of nozzle, thus influencing the droplet diameter of the electrosprayed particles.[25]

We further examined the role of ELP concentration on electrospray morphology for this ELP. Figure 5 shows SEM images of electrosprayed ELP particles using a solution concentration of 0.5 w/v% with other parameters identical to those used in Figure 4. Figure 5a–c show the ELP particles produced at a flow rate of 0.05 mL/h and a spraying voltage of 7, 8, and 9 kV. It can be seen from Figure 5a–c that the average particle size decreased slightly with an increase in the spraying voltage, producing hollow particles. The hollow particles were larger in diameter than the solid particles generated with similar masses. The particle sizes were distributed over an approximate range of 20−743 nm. When the flow rate was increased to 0.1 mL/h, ELP particles with collapsed surfaces were generated, as shown in Figure 5d–f. The SEM images demonstrated that the morphologies of the ELP particles were not uniform and spherical. The formation of collapsed surface and hollow particles correlated to a lower solution concentration and a lower molecular weight. Figures 4 and 5 show that the ELP particles electrosprayed using

a solution concentration of 1 w/v% had smooth, spherical morphologies, whereas the particles generated using a solution concentration of 0.5 w/v% were ladle type structures.

The results obtained from these experiments highlight the role of different variables in the formation of electrosprayed ELP particles. We found that the solution concentration played an important role in determining ELP particle morphology. The ELP molecular weight also had a significant and independent effect on the morphology of the ELP particles, as decreasing the molecular weight of the ELP biopolymers resulted in a change in the particle morphologies from fibers and particles with tails to completely spherical particles. The solution viscosity is a function of the molecular weight due to the chain entanglements in the solution, so a 4-fold increase in the molecular weight increases the extensional viscosity by 2−3 orders of magnitude.[26] Higher viscosity promotes the formation of tails or fibrous structures under different processing conditions. In contrast, the use of low molecular weight ELPs reduces the surface tension and the viscosity, leading to the formation of smooth and spherical ELP particles. These results are consistent with a previous study relating polymer properties and particle morphology.[27]

Based on the above results, a set of “optimal” processing parameters was used to prepare spherical drug-loaded ELP particles, using the low MW ELP (Table 1). To codissolve ELP and Dox for electrospraying, Dox was dissolved in a mixture of trifluoroethanol and ethanol (25:1 v/v). The Dox solution was then added to ELPs dissolved in trifluoroethanol. The concentrations of ELPs were 0.5 w/v% and 1.0 w/v%. The concentration of Dox in the solution was 20 w/w% of the ELP biopolymer mass. ELPs that follow the Val-Pro-Gly-Xaa-Gly motif have not been reported to undergo irreversible denaturation, and most ELP phase transitions are reversible even after prolonged exposure to high temperatures.[15] While ELPs are compatible with organic solvents like trifluoroethanol, the use of this protocol to encapsulate folded protein drugs will require additional study.

Figure 6a,b shows an SEM image of ELP-Dox particles tested for the release of drug and their particle size distribution, respectively. The electrosprayed particles had spherical and smooth morphologies, with a narrow particle size distribution as shown in Figure 6b. The particle diameters were distributed over a range of 150−570 nm, with an average particle size of 370 ± 25 nm. About 50% of the particles were between 300 and 400 nm in diameter.

The ELP transition temperatures in solution were a function of both concentration and pH (Figure 7a), so that changing the solution pH was a convenient method to isothermally modulate the LCST driven solubility of the ELP and its concomitant effect on the release of Dox from the ELP particles.

Figure 7a illustrates the pH-dependent transition temperatures of the 17.8 kD ELP used to generate drug-loaded particles. At pH 7.5, no transitions were observed below 90 °C. At concentrations greater than 50 μM and pH 6.5, ELPs transitioned below 90 °C but significantly greater than 37 °C. At pH 2.5, glutamic acid side chains on the ELPs protonated and became charge neutral. Neutral residues were more hydrophobic, and this decreased the transition temperature below 37 °C at pH 2.5 and 3.5. Hence, particles exposed to pH 6.5 and 7.5 should rapidly dissolve in water, while the particles incubated in pH 2.5 would be expected to exist as a coacervate phase. ELPs follow a linear relationship between the transition temperature and the logarithm of the concentration;[6] therefore, for pH where data was observable, below 95 °C, a best fit regression and corresponding 95% confidence interval have been presented (Figure 7a).

The pH-mediated release of Dox from the electrosprayed ELP particles was investigated to examine the role of ELP solubility on Dox release. As electrospraying is an evaporative process, both polymer and drug are conserved during drug encapsulation. Thus, the ratio of drug to

polymer in the deposited nanoparticles is expected to be similar to that of the mixture 20% by weight drug. We postulated that drug release would depend on ELP solubility, as defined by the transition temperature. To explore this hypothesis, the release of Dox from ELP nanoparticles was observed at 37 °C at pH values that promote coacervation (pH 2.5), solubility (pH 7.5), or intermediate behavior (pH 5.5) (Figure 7b). ELP Dox nanoparticles attached to a silica surface (2 × 2 mm) were incubated in solutions of different pH conditions. Silica pieces had an average weight of 13.6 ± 1.4 mg, and the encapsulation efficiency for recoverable Dox was 7.1 ± 3.0 picomoles Dox/mg silica (n = 12).

The differences between the cumulative release of Dox from ELP particles in the coacervate (pH 2.5) and soluble phases (pH 5.5, 7.5) were significant after 1 h (R^2 = 0.77, $F_{2,6}$ = 10.1, p = 0.012). Particles incubated at high pH (5.5, 7.5) and 37 °C, below their transition temperature, displayed nearly complete release of Dox after only 15 min. In contrast, particles incubated at pH 2.5 and 37 °C, above their transition temperature, reached a plateau of only ~70% released Dox. The other ~30% of drug remained trapped in the ELP coacervate but could be released upon return to solubility at pH 7.5. All particles displayed an initial burst of Dox; however, the pH 2.5 treated particles experienced the lowest burst with an average 47 ± 13% release at time zero. This initial burst may have been due to the fact that ELP coacervates contain significant water under equilibrium.[15] Thus, upon immersion in buffer, electrosprayed ELPs imbibe water. This intake of water into dehydrated ELPs may facilitate a burst release of Dox, as water diffuses into the entangled mass of polymer. For particles below their transition temperature, this process proceeds to complete solubility and release of drug, while particles above the transition temperature retain a portion of drug in the coacervate phase for extended periods. These results suggest that isothermal mechanisms for manipulating ELP phase transition may be useful for achieving controlled drug release.

4. Conclusions

In summary, we demonstrated the fabrication of ELP particles for drug delivery through electrospraying of an organic solution of the biopolymer. The molecular weight of ELP and the concentration of solution had a significant influence on the morphologies of electrosprayed ELP particles. Higher flow rates and lower spraying voltages resulted in the formation of particles with tail structures and fibers along with spherical particles. Spherical particles could easily be generated from ELP polymers with a low molecular weight. We evaluated the encapsulation and triggered release of a model drug, Dox, from ELP particles and observed that the release of Dox from pH responsive particles followed the pH-dependent solubility of the ELP. These results demonstrate that electrospraying is a versatile technique for generating spherical ELP particles that have potential for drug delivery.

Acknowledgments

This work was supported with NIH Grant 5F32-CA-123889 to J.A.M. and NIH Grant R01-EB-00188 to A.C. We thank K. Fitzgerald for synthesizing genes for this study.

References and Notes

1. Wu YQ, Clark RL. Controllable Porous Polymer Particles Generated by Electrospraying. J. Colloid Interface Sci 2007;310(2):529–535. [PubMed: 17346734]
2. Wu YQ, Clark RL. Electrohydrodynamic Atomization: A Versatile Process for Preparing Materials for Biomedical Applications. J. Biomater. Sci., Polym. Ed 2008;19(5):573–601. [PubMed: 18419939]
3. Wu, YQ.; Clark, RL. Handbook of Fabrication and Processing of Biomaterials. CRC Press/Taylor and Francis Group; Boca Raton, FL: 2008. Electrohydrodynamic Processing of Micro- and Nanometer Biomaterials.; p. 275-333.

4. Blum RH, Carter SK. Adriamycin-New Anticancer Drug with Signigicant Clinical Activity. Ann. Intern. Med 1974;80(2):249–259. [PubMed: 4590654]
5. Dimarco A, Gaetani M. Adriamycin (Nsc-123127)—A New Antibiotic with Antitumor Activity. Cancer Chemother. Rep 1969;53(1):33–37. [PubMed: 5772652]
6. Meyer DE, Chilkoti A. Quantification of the Effects of Chain Length and Concentration on the Thermal Behavior of Elastin-Like Polypeptides. Biomacromolecules 2004;5(3):846–851. [PubMed: 15132671]
7. Trabbic-Carlson K, Setton LA, Chilkoti A. Swelling and Mechanical Behaviors of Chemically Cross-Linked Hydrogels of Elastin-Like Polypeptides. Biomacromolecules 2003;4(3):572–580. [PubMed: 12741772]
8. Yamaoka T, Tamura T. Mechanism for the Phase Transition of a Genetically Engineered Elastin Model Peptide (VPGIG)(40) in Aqueous Solution. Biomacromolecules 2003;4(6):1680–1685. [PubMed: 14606895]
9. Herrero-Vanrell R, Rincon AC, Alonso M. Self-Assembled Particles of an Elastin-Like Polymer as Vehicles for Controlled Drug Release. J. Controlled Release 2005;102(1):113–122.
10. Dreher MR, Raucher D, Balu N. Evaluation of an Elastin-Like Polypeptide-Doxorubicin Conjugate for Cancer Therapy. J. Controlled Release 2003;91(1−2):31–43.
11. Dreher MR, Liu WG, Michelich CR. Tumor Vascular Permeability, Accumulation, and Penetration of Macromolecular Drug Carriers. J. Natl. Cancer Inst 2006;98(5):335–344. [PubMed: 16507830]
12. Furgeson DY, Dreher MR, Chilkoti A. Structural Optimization of a “Smart” Doxorubicin—Polypeptide Conjugate for Thermally Targeted Delivery to Solid Tumors. J. Controlled Release 2006;110(2):362–369.
13. Chilkoti A, Dreher MR, Meyer DE. Design of Thermally Responsive, Recombinant Polypeptide Carriers for Targeted Drug Delivery. Adv. Drug Delivery Rev 2002;54(8):1093–1111.
14. Dreher MR, Liu WG, Michelich CR. Thermal Cycling Enhances the Accumulation of a Temperature-Sensitive Biopolymer in Solid Tumors. Cancer Res 2007;67(9):4418–4424. [PubMed: 17483356]
15. Urry DW. Physical Chemistry of Biological Free Energy Transduction as Demonstrated by Elastic Protein-Based Polymers. J. Phys. Chem. B 1997;101(51):1007–28.
16. Meyer DE, Chilkoti A. Purification of Recombinant Proteins by Fusion with Thermally-Responsive Polypeptides. Nat. Biotechnol 1999;17(11):1112–1115. [PubMed: 10545920]
17. Kriger MS, Cook KD, Ramsey RS. Durable Gold-Coated Fused-Silica Capillaries for Use in Electrospray Mass Spectrometry. Anal. Chem 1995;67(2):385–389. [PubMed: 7856882]
18. Tang K, Gomez A. Generation by Electrospray of Monodisperse Water Droplets for Targeted Drug-Delivery by Inhalation. J. Aerosol Sci 1994;25(6):1237–1249.
19. Ku BK, Kim SS. Electrohydrodynamic Spraying Characteristics of Glycerol Solutions in Vacuum. J. Electrost 2003;57(2):109–128.
20. Li JL, Tok A. Electrospraying of Water in the Cone-Jet Mode in Air at Atmospheric Pressure. Int. J. Mass Spectrom 2008;272(2−3):199–203.
21. Lopez-Herrera JM, Barrero A, Boucard A, Loscertales IG, Marquez M. An Experimental Study of the Electrospraying of Water in Air at Atmospheric Pressure. J. Am. Soc. Mass Spectrom 2004;15(2):253–259. [PubMed: 14766292]
22. Noakes, TJ. European Patent No. 0 468 736 B1
23. Zhang CX, Yuan XY, Wu LL. Study on Morphology of Electrospun poly(vinyl alcohol) Mats. Eur. Polym. J 2005;41(3):423–432.
24. Koski A, Yim K, Shivkumar S. Effect of Molecular Weight on Fibrous PVA Produced by Electrospinning. Mater. Lett 2004;58(3−4):493–497.
25. GananCalvo AM, Davila J, Barrero A. Current and Droplet Size in the Electrospraying of Liquids. Scaling Laws. J. Aerosol Sci 1997;28(2):249–275.
26. Yu JH, Fridrikh SV, Rutledge GC. The Role of Elasticity in the Formation of Electrospun Fibers. Polymer 2006;47(13):4789–4797.
27. Shenoy SL, Bates WD, Frisch HL. Role of Chain Entanglements on Fiber Formation During Electrospinning of Polymer Solutions: Good Solvent, Non-Specific Polymer—Polymer Interaction Limit. Polymer 2005;46(10):3372–3384.

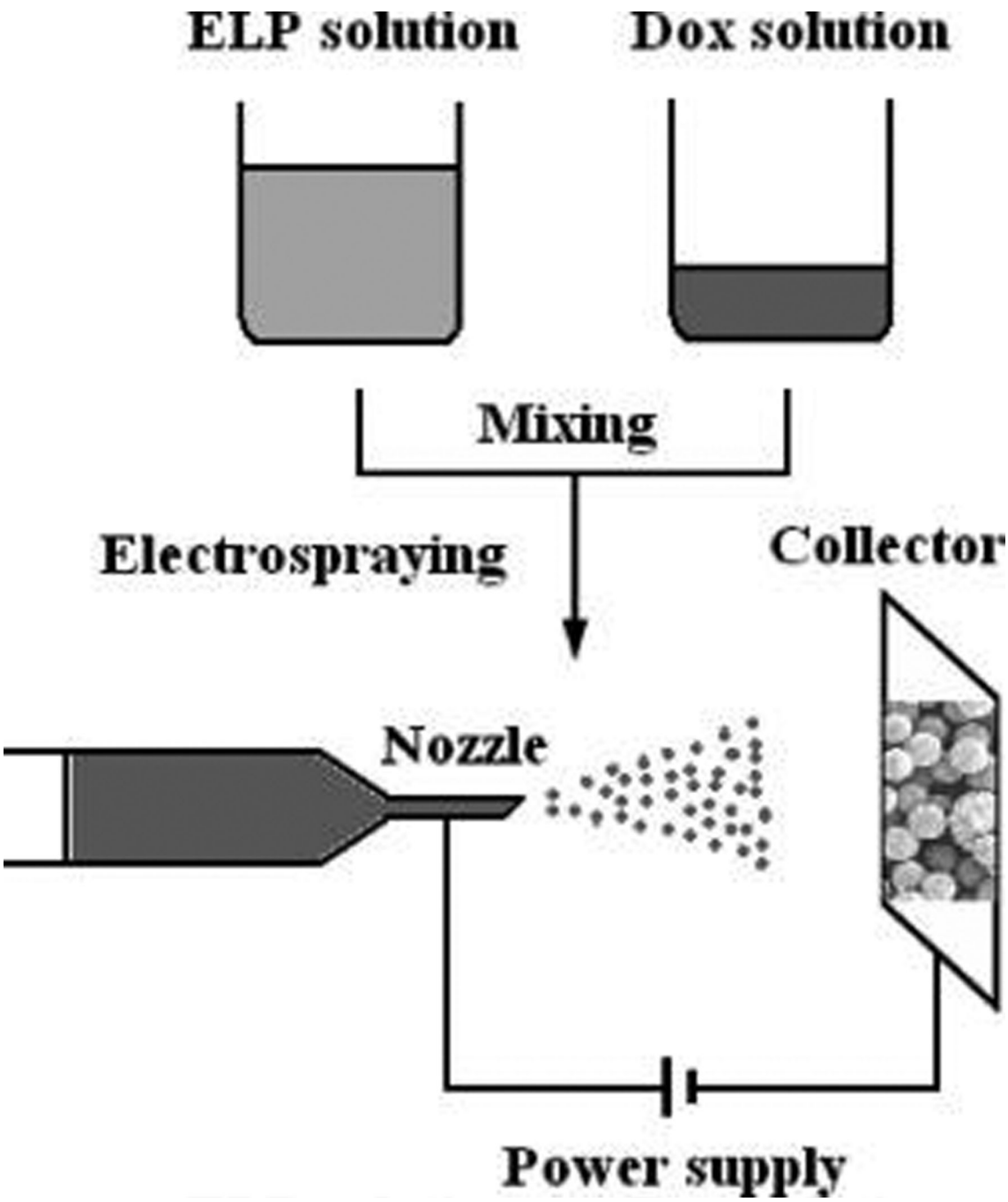

Figure 1.
Schematic diagram of an electrospraying setup for preparing ELP drug delivery particles.

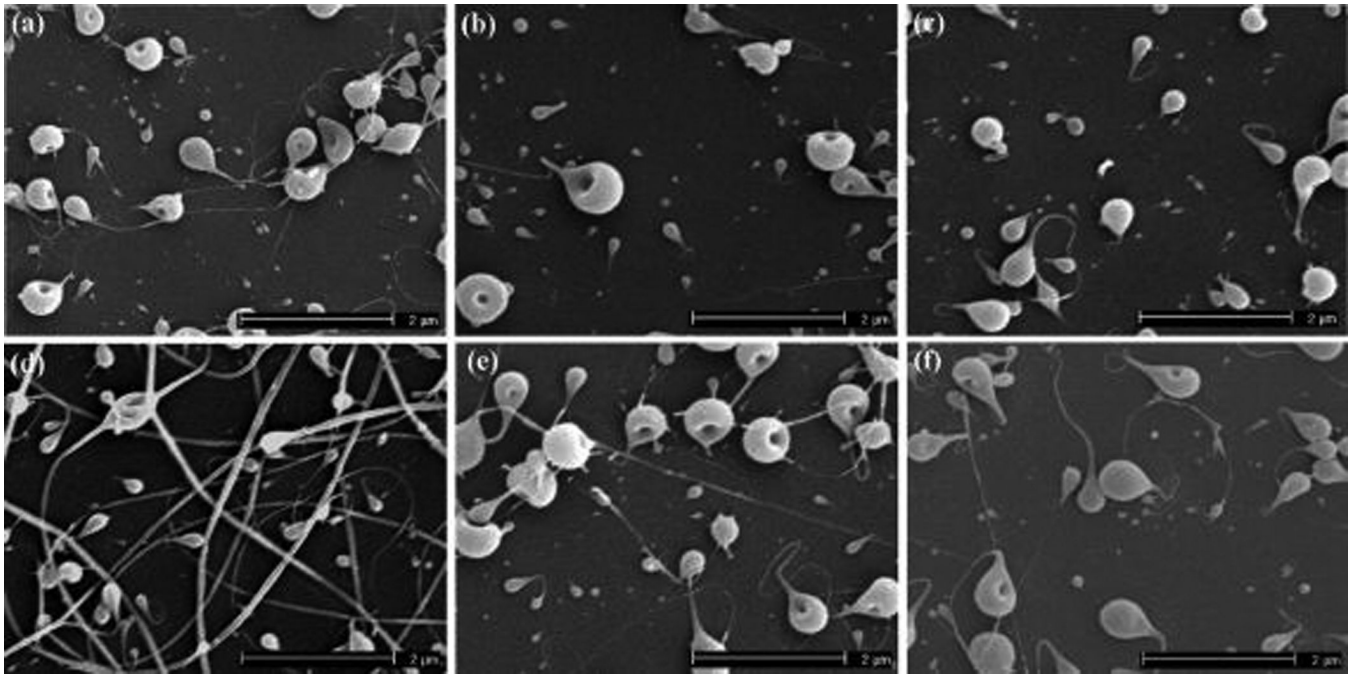

Figure 2.
SEM images of electrosprayed ELP particles prepared using a molecular weight of 70.2 kD and a solution concentration of 1 w/v% at (a) *V*: 7 kV and *F*: 0.05 mL/hr; (b) *V*: 8 kV and *F*: 0.05 mL/hr; (c) *V*: 9 kV and *F*: 0.05 mL/hr; (d) *V*: 7 kV and *F*: 0.1 mL/hr; (e) *V*: 8 kV and *F*: 0.1 mL/hr; (f) *V*: 9 kV and *F*: 0.1 mL/hr [*V*: spraying voltage and *F*: flow rate].

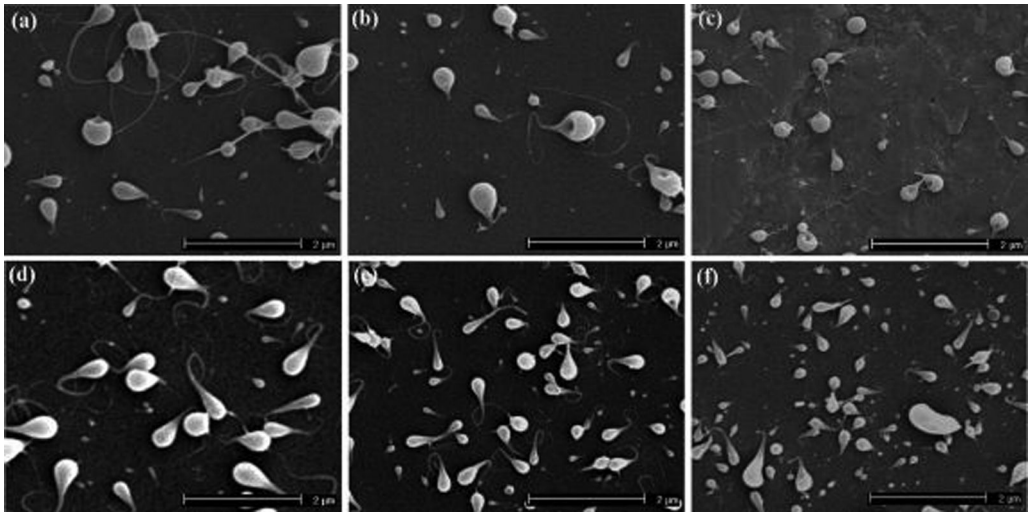

Figure 3.

SEM images of electrosprayed ELP particles prepared using a molecular weight of 70.2 kD and a solution concentration of 0.5 w/v% at (a) *V*: 7 kV and *F*: 0.05 mL/hr; (b) *V*: 8 kV and *F*: 0.05 mL/hr; (c) *V*: 9 kV and *F*: 0.05 mL/hr; (d) *V*: 7 kV and *F*: 0.1 mL/hr; (e) *V*: 8 kV and *F*: 0.1 mL/hr; (f) *V*: 9 kV and *F*: 0.1 mL/hr [*V*: spraying voltage and *F*: flow rate].

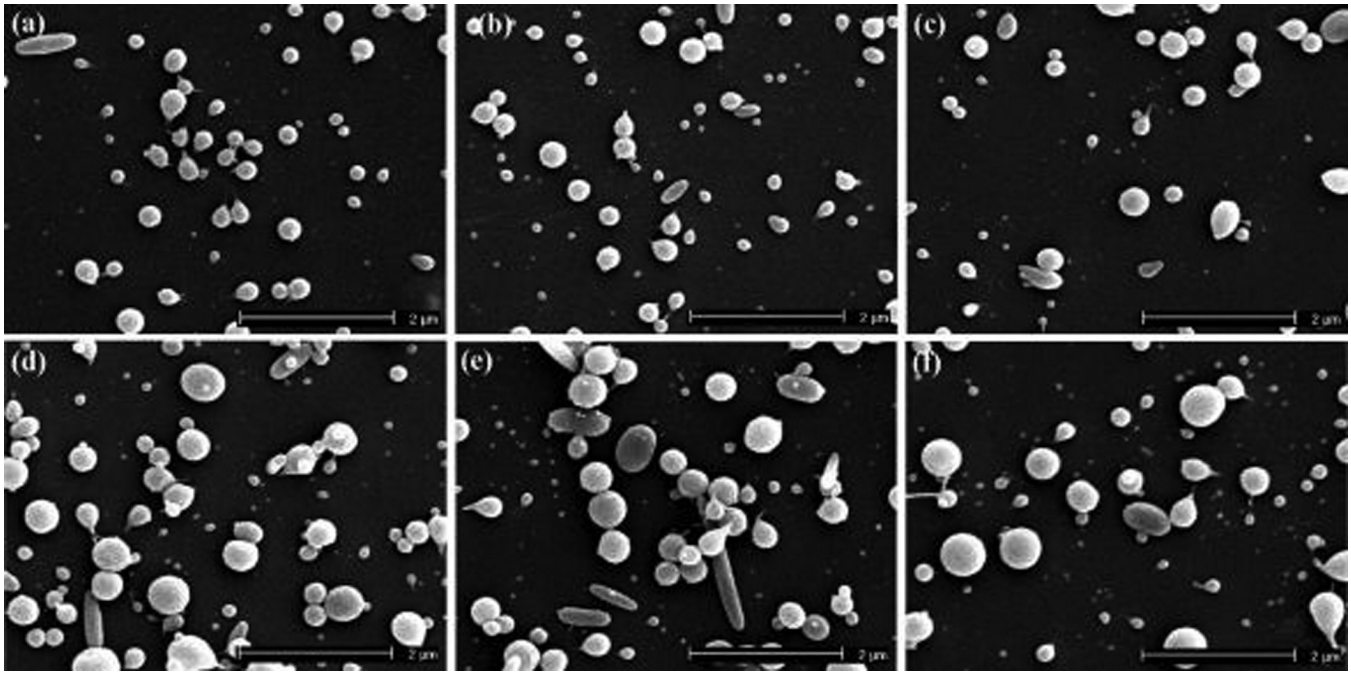

Figure 4.
SEM images of electrosprayed ELP particles prepared using a molecular weight of 17.8 kD and a solution concentration of 1 w/v% at (a) *V*: 7 kV and *F*: 0.05 mL/hr; (b) *V*: 8 kV and *F*: 0.05 mL/hr; (c) *V*: 9 kV and *F*: 0.05 mL/hr; (d) *V*: 7 kV and *F*: 0.1 mL/hr; (e) *V*: 8 kV and *F*: 0.1 mL/hr; (f) *V*: 9 kV and *F*: 0.1 mL/hr [*V*: spraying voltage and *F*: flow rate].

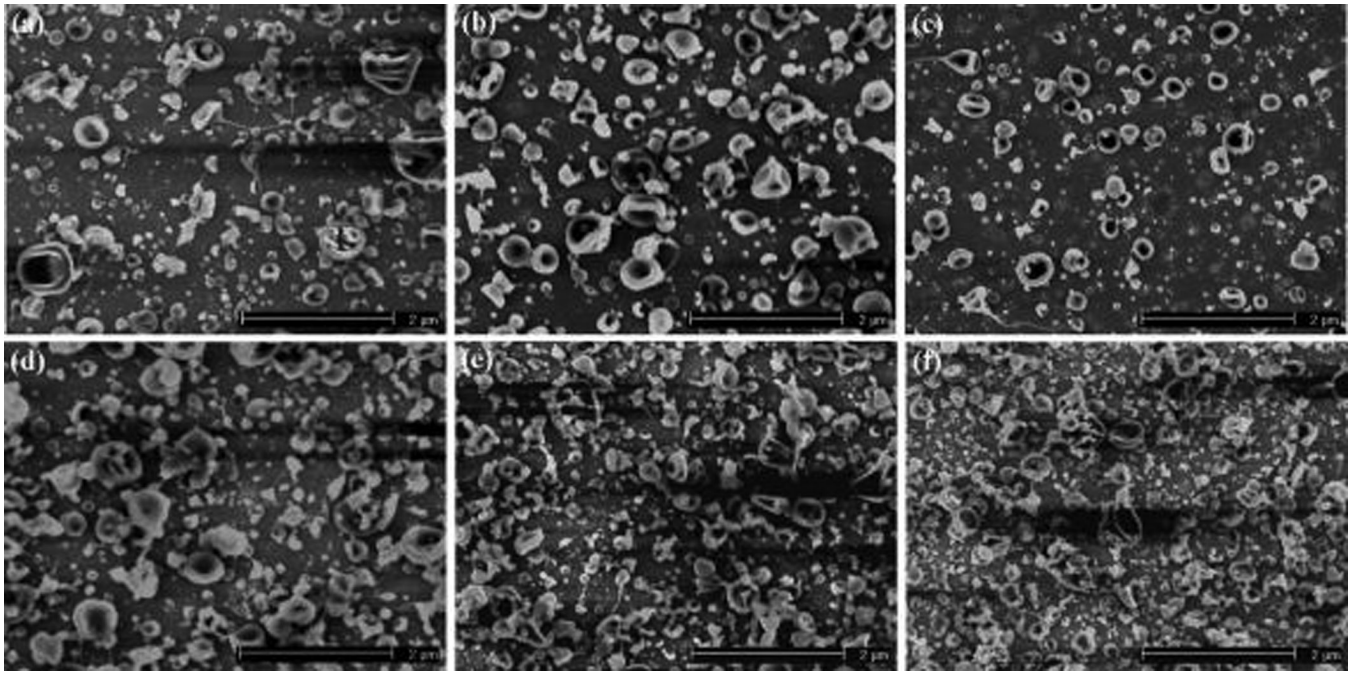

Figure 5.
SEM images of electrosprayed ELP particles prepared using a molecular weight of 17.8 kD and a solution concentration of 0.5 w/v% at (a) *V*: 7 kV and *F*: 0.05 mL/hr; (b) *V*: 8 kV and *F*: 0.05 mL/hr; (c) *V*: 9 kV and *F*: 0.05 mL/hr; (d) *V*: 7 kV and *F*: 0.1 mL/hr; (e) *V*: 8 kV and *F*: 0.1 mL/hr; (f) *V*: 9 kV and *F*: 0.1 mL/hr [*V*: spraying voltage and *F*: flow rate].

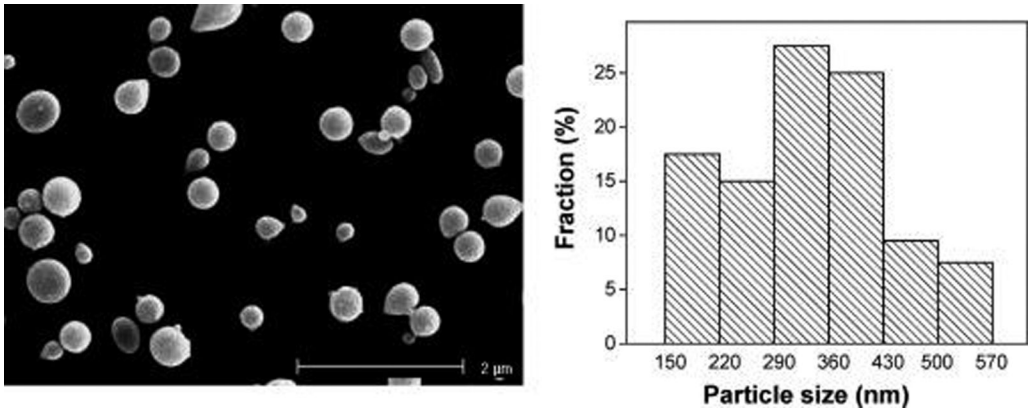

Figure 6.
(a) SEM image and (b) particle size distribution of electrosprayed Dox-loaded ELP particles.

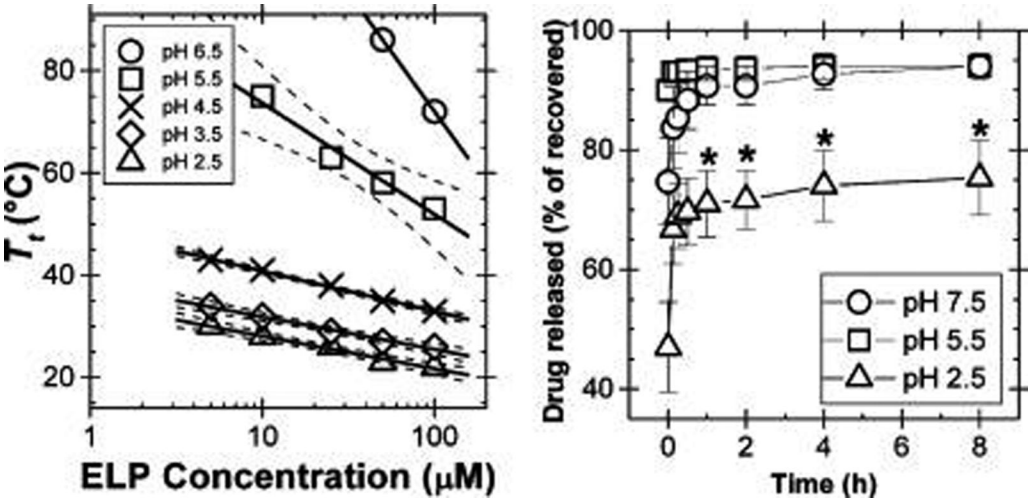

Figure 7.

(a) pH-dependent transition temperatures of 17.8 kD ELPs as a function of concentration at pH 6.5 (circle), 5.5 (square), 4.5 (cross), 3.5 (diamonds), and 2.5 (triangle). A best-fit line and 95% confidence interval are presented. Fit model: $T_t = m \text{ Log}_{10}(C_{ELP}) + b$. (b) Cumulative drug release from 17.8 kD ELP nanoparticles at 37 °C. Error bars indicate standard error (n = 3). *Significant ($p < 0.05$, ANOVA-Tukey) difference in comparison to either pH 7.5 or 5.5.

Table 1

Processing Parameters for Electrospinning ELP Particles

electrospraying parameters	**data**
applied voltage	8 kV
flow rate	0.1 mL/hr
working distance	40 cm
molecular weight	17.8 kD
concentration	1 w/v%